Journal of Materials Chemistry A

Accepted Manuscript

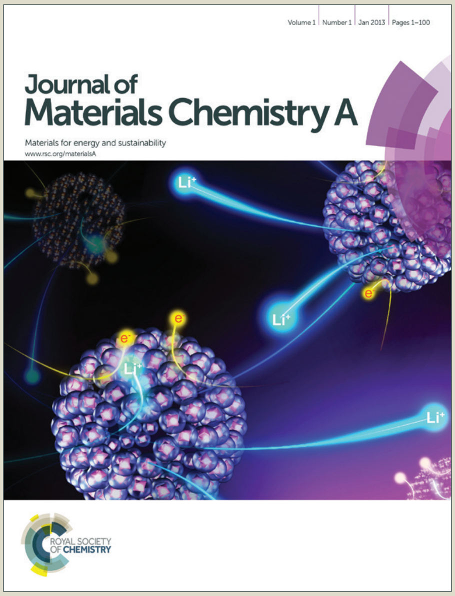

ROYAL SOCIETY OF CHEMISTRY

www.rsc.org/materialsA

Journal Name

COMMUNiCATION

MOF-derived surface modified Ni nanoparticles as an efficient catalyst for the hydrogen evolution reaction

Received 00th January 20xx,
Accepted 00th January 20xx

DOI: 10.1039/x0xx00000x

www.rsc.org/

Teng Wang,[a] Qianyu Zhou, [a] Xiaojuan Wang, [a] Jie Zheng* [a] and Xingguo Li* [a]

Pyrolysis of a Ni based metal organic framework in NH_3 yields Ni nanoparticles with surface nitridation together with thin carbon coating layers. The subtle surface modification significantly improves the catalytic performance for the hydrogen evolution reaction (HER). The surface modified Ni nanoparticles shows a low overpotential of only 88 mV at current density 20 mA cm^{-2}, which is one of the most efficient HER catalysts based on metallic Ni reported so far. The results suggest that controlled pyrolysis of MOFs is an effective method to prepare highly efficient noble metal free HER catalysts.

Broader context

Water electrolysis can generate hydrogen in a renewable way, which now also serves as an important energy storage solution for the renewable energy source such as wind power or photovoltaics. Cheap yet efficient catalysts for the hydrogen evolution reaction (HER) are of critical importance to support the renewable hydrogen generation from water electrolysis with high energy efficiency. Nickel is a cheap HER catalyst and is widely used in current alkaline electrolyzers. However, it is generally regarded less efficient. Here we demonstrate that a Ni based catalyst obtained by pyrolysis of a Ni based metal organic framework in NH_3 shows very high HER efficiency. The catalyst is composed of Ni nanoparticles with surface nitridation and thin carbon layer coating. The results will advance the development of Ni based efficient yet low cost HER catalysts. The significant improvement in HER performance caused by the subtle surface modification is also of fundamental interest for catalysis.

Introduction

Hydrogen is a promising clean energy solution to replace fossil fuels. The true merit of hydrogen as a zero emission energy source can only be achieved if hydrogen can be obtained in a sustainable way. Water electrolysis is a well-known method to produce hydrogen, which is regaining increasing interest in recent years. [1-3] Hydrogen generation by water electrolysis can serve as a promising energy storage solution for the intermittent wind or solar electric power. By combining wind power or photovoltaics, electrolysers and hydrogen fuel cells, distributed electricity generation that is truly independent of grids can be achieved[4-7] .

Efficient electrocatalysts for the hydrogen evolution reaction (HER) are required to promote the electricity-to-hydrogen conversion efficiency. Currently, the noble metals, especially platinum, remain the most efficient HER catalysts, which exhibit both very low overpotential and very good stability. However, the low abundance and high expense of Pt limits its application in large-scale water electrolysis. Therefore, developing efficient noble-metal-free catalysts for HER is of critical importance to support the widespread electrochemical hydrogen production.

As a common low cost alternative for Pt in many catalytic reactions, Ni based electrodes are extensively used in current commercial alkaline electrolysers. Improving the efficiency of Ni based catalysts, therefore, may results in direct impact on the current alkaline electrolysis technology. Ni is inherently much less efficient for HER compared to Pt-based catalysts. [8, 9] To enhance the efficiency of Ni based HER catalysts, a large variety of Ni based alloys or intermetallic composites are studied, such as Ni-Mo[8, 10], Ni-Cu[11], Ni-Cr[12], and Ni-Co[13, 14]. Ni compounds with non-metal elements, such as O or OH[15, 16], P[17, 18] and S[19-21] have also been reported to show improved HER performance. On the other hand, metallic Ni is generally considered much less active. Consequently, HER catalysts based on metallic Ni are much less studied in recent years.

Here we report a highly efficient HER catalyst based on surface modified Ni nanoparticles derived from a Ni-based metal organic frameworks (MOFs). Pyrolysis of the Ni-MOF, $Ni_2(bdc)_2ted$ (bdc = 1,4-benzenedicarboxylic acid; ted = triethylene-diamine), in NH_3 results in Ni nanoparticles with

---

[a] Beijing National Laboratory for Molecular Sciences (BNLMS), (The State Key Laboratory of Rare Earth Materials Chemistry and Applications), College of Chemistry and Molecular Engineering, Peking University, Beijing, 100871, China. E-mail: zhengjie@pku.edu.cn; xgli@pku.edu.cn.

Electronic Supplementary Information (ESI) available: Experimental details, characterization of the MOF, additional XRD, TEM and electrochemical measurements. See DOI: 10.1039/x0xx00000x surface nitridation together with thin carbon layer coating. The surface modification significantly improves the HER performance. The catalyst exhibits low overpotential of only 88 mV at current density 20 mA cm^{-2} in, which is one of the most efficient HER catalysts based on metallic Ni reported so far.

In recent years, there is an increasing interest in preparing metal containing functional materials by pyrolysis of MOFs, which have shown promising application in electric energy storage and electrocatalysis[22-25]. MOFs are advantageous as precursors to derive functional materials for their highly ordered spatial arrangement of the metal cations with well defined chemical environment. In most studies, the pyrolysis is carried out in inert atmosphere. Here, NH_3 is introduced during the pyrolysis process, which is critical to yield the desired surface state for HER by removing the excessive carbon and assisting surface nitridation. The improved pyrolysis procedure will assist the development of efficient HER catalysts from MOFs, which is currently significantly underdeveloped[26] compared to other applications of MOF derived materials.

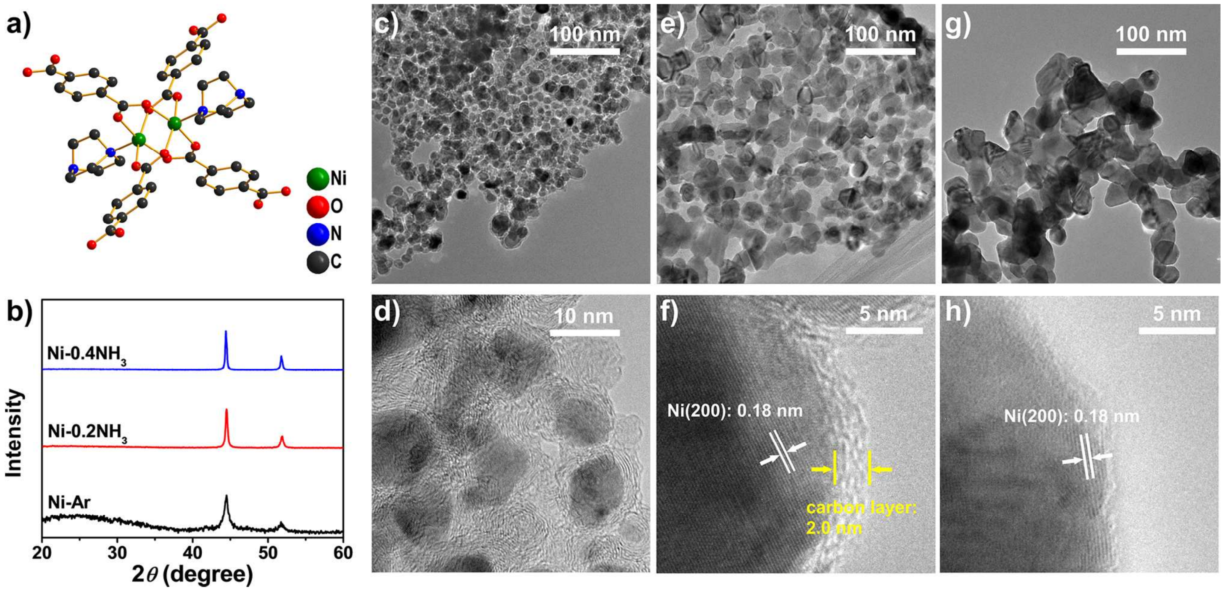

Fig. 1 a) The structure of the Ni coordination environment in $Ni_2(bdc)_2(ted)$, b) XRD patterns of the Ni-MOF derived catalysts, c)-h) TEM images of the Ni-MOF derived catalysts: c) & d) Ni-Ar, e) & f) Ni-0.2-NH_3, g) & h) Ni-0.4NH_3.

Results and discussion

The Ni-MOF is synthesized by a solvothermal method following previous publications[27, 28]. $Ni(NO_3)_2 \cdot 6H_2O$, H_2bdc and ted are dissolved in dimethylformamide and sealed in an autoclave and kept at 130 °C for 24 h. The Ni-MOF precipitates as green fine crystals which can be easily separated by filtration. The Ni-MOF is well crystallized with high specific surface area of 2085 m^{2}g^{-1}. The size of the Ni-MOF crystals ranges from 0.2 to several micrometers (Fig. S1). The Ni-MOF shows a layer-pillar structure. Each Ni atom is coordinated by four oxygen atoms from bdc and one nitrogen atom from ted (Fig. 1a).

The catalysts are prepared by pyrolysis of the Ni-MOF at 560 °C in different atmosphere for 1h. The Ni-MOF completely decomposes above 500 °C in inert atmosphere, as suggested by the thermal gravimetric analysis (Fig. S1d). Table 1 summarizes the composition of the catalysts obtained in different pyrolysis atmosphere. All the samples are composed of Ni, C and N. X-ray diffraction (XRD, Fig. 1b) confirms that metallic Ni is the only crystalline phase in all the samples, indicating that most Ni is in the metallic state. A notable feature is that NH_3 introduced during the pyrolysis significantly reduces the carbon content. The carbon content is more than 30 wt% for the Ni-Ar sample while is only 1.22 wt% for the Ni-0.2NH_3 sample. Increase the NH_3 partial pressure to 0.4 bar almost eliminates carbon.

Table 1. The compositions and specific surface area (S_{BET}) of the MOF-derived catalysts

sample	atmosphere	C (wt%)	N (wt%)	Ni (wt%)	S_{BET} (m^2/g)
Ni -Ar	Ar	30.86	2.63	52.8	128.2
Ni -0.2NH_3	20%NH_3 in Ar	1.22	0.67	94.9	18.3
Ni -0.4NH_3	40%NH_3 in Ar	0.26	0.19	96.1	18.1
Ni -0.2H_2	20% H_2 in Ar	30.56	0.61	62.2	165.2
Ni-Ar-0.2NH_3	Ar then 20%NH_3 in Ar	31.1	2.80	59.6	121.1

Transmission electron microscopy (TEM) shows that the Ni-Ar sample is composed of Ni nanoparticles less than 10 nm in diameter homogeneously distributed in a continuous carbon matrix (Fig. 1c). The carbon matrix is largely amorphous, while graphitic layers can be observed near the Ni particles (Fig. 1d).

Such structure with metal nanoparticles embedded in a carbon matrix is commonly observed in the pyrolysis products of MOFs in inert atmosphere.[29-31]

For catalysts obtained in NH_3, a notable structural difference is the absence of the continuous carbon matrix. The Ni-0.2NH_3 sample contains only very thin carbon layers (~2 nm) coating on the surface of the Ni particles (Fig 2f), while the Ni-0.4NH_3 sample shows almost no carbon coating (Fig 2h). This is in agreement with the very low carbon content obtained by the elemental analysis (Table 1). Another difference is the slightly larger particle size of Ni. Both samples obtained in NH_3 atmosphere contain Ni particles around 30-50 nm (Fig. 2e and 2g). Both samples have a low BET surface area of 18 m^2 g^{-1} (Table 1), which gives average diameter 18 nm of the Ni particles, in very good agreement with the TEM results.

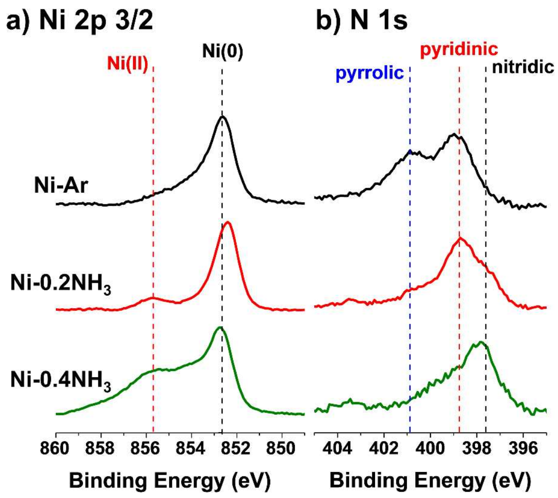

Fig. 2 a) Ni 2p 3/2 and b) N 1s XPS spectra of MOF-derived catalysts. The shake-up peaks of Ni 2p 3/2 have been subtracted for clarity.

Fig. 2 shows the XPS spectra of the catalysts. In the Ni 2p$_{3/2}$ spectra, the peak at 852.7±0.2 eV corresponding to metallic Ni is observed for all the samples, which is in agreement with the XRD and TEM results. Samples obtained in NH_3 contain another peak at 856 eV corresponding to divalent Ni[32, 33]. In the N 1s spectra, components corresponding to pyridinic (398.9 eV), pyrrolic (400.9 eV) and graphitic (402.8 eV) nitrogen [22, 32, 34]can be identified for all the samples, which are commonly found in N-doped carbon[22, 35, 36]. Samples obtained in NH_3 contain another component with binding energy lower than 398 eV, which can be identified as electron-rich nitridic nitrogen[34]. It is worth noting that higher NH_3 partial pressure during pyrolysis results in higher relative abundance of both the divalent Ni and the nitridic N, which suggests partial nitridation of the Ni particles occurs in these samples. Another indirect evidence for the partial nitriation of Ni is the extremely high N/C ratio in samples obtained in NH_3 (Table 1). Considering the very low nitrogen content and the absence of crystalline nickel nitride phase in XRD, the nitridation is likely to occur only on the surface of the Ni particles.

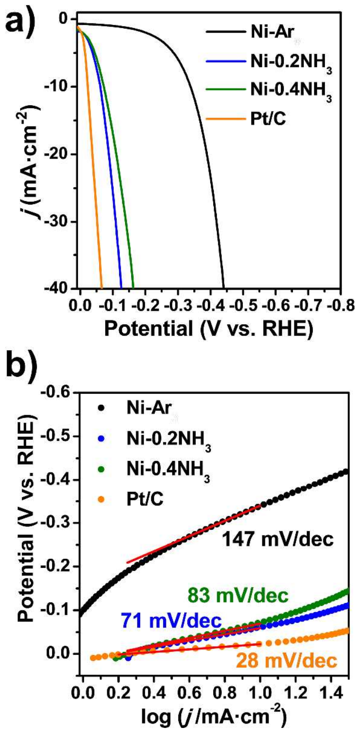

Fig. 3 a) Linear scanning voltammetry and b) Tafel plots of the MOFs-derived catalysts in 1M KOH solution.

The HER performance of the catalysts is first evaluated by the linear scanning voltammetry (LSV, Fig. 3a). The activity is compared using the overpotential at certain current density j (η_j, j in mA cm^{-2}). Notably, the Ni-0.2NH_3 sample shows very high HER activity, indicated by the low overpotential (η_{10}= 61 mV and η_{20}=88 mV). The HER performance, however, is very sensitive to the NH_3 partial pressure during pyrolysis. The performance of the Ni-0.4NH_3 sample is inferior (η_{20} = 112 mV). The Ni-Ar sample is rather inactive (η_{20}= 390 mV).

These Ni-MOF derived catalysts also exhibit different HER mechanisms, which can be inferred from the Tafel plots (Fig 3b). The Tafel slope for the catalysts derived in NH_3 is in the range of 71-83 mV/decade, which suggests a mixed Volmer and Heyrovsky mechanism for HER, i.e. the HER rate is determined by both H_2O discharge and desorption of H from the catalyst surface[14, 37-39]. For the Ni-Ar catalyst, the Tafel slope is much higher (147 mV/decade), suggesting that the HER is dominated by the Volmer mechanism, i.e. determined by the discharge of H_2O[1, 37, 39].

The most active catalyst Ni-0.2NH_3 also shows very good stability. As shown in Fig. 4a, during a continuous water electrolysis test at constant current of 20 mA·cm^{-2}, the overpotential only slightly increases from 91 mV to 103 mV in 12 h(Fig. 4a). The catalyst after electrolysis shows no apparent change in terms of the particle size and the morphology of carbon layer (Fig. 4b), which can be attributed to the good protection of the surface carbon layer. The LSV profile is also unaffected after repeated cyclic voltammetry scans (Fig. S4). The H_2 evolved measured by chromatography shows excellent linear dependence with time during the constant current electrolysis (Fig. 4c). The moles of H_2 equals half of the moles of electrons passing through the electrolysis cell within the measurement error, indicating near 100% Faraday efficiency throughout the continuous electrolysis test.

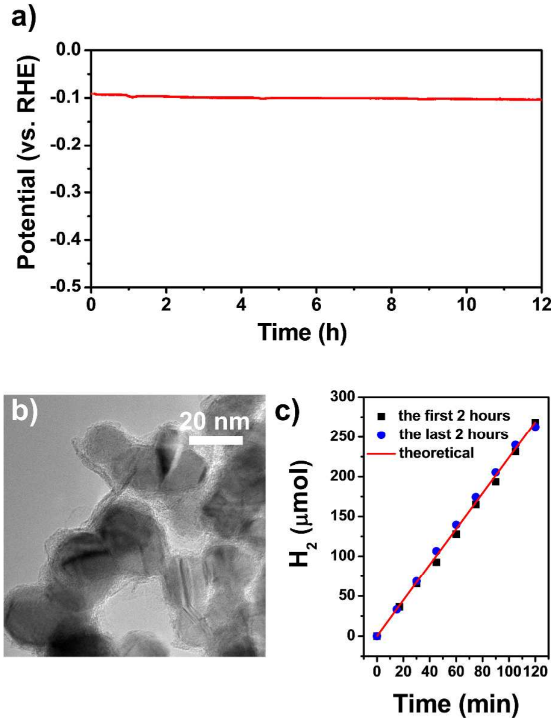

Fig 4. a) Chronopotentiometry of the Ni-0.2NH_3 sample at constant current density 20 mA cm^{-2}. The electrode is prepared by loading the catalyst on a Ni foam. The contribution to the current from the Ni foam is less than 5% (Fig. S4). b) TEM image of the catalyst after continuous operation for 12 h. c) The amount of H_2 generated by electrolysis in the first and last 2 hours, which is in excellent agreement with the theoretical value assuming 100% Faraday efficiency (the straight line).

Table S1 compares the performance of our Ni-MOF derived catalyst with several state of the art Ni based noble metal free HER catalysts. Metallic Ni (e.g. Ni particles obtained by chemical reduction) typically show η_{10}> 300 mV[8, 40]. Most nickel based alloys and compounds reported in literature have η_{20}> 100 mV[17, 18, 41]. There are only very few Ni based noble metal free HER catalysts exhibit η_{20} below 100 mV[8, 16]. The Ni-0.2NH_3 catalyst, therefore, represents a significant improvement in the HER activity of Ni based HER catalysts. Considering the fact that this catalyst is not much different compared to ordinary Ni nanoparticles except the surface state, such improvement is even more intriguing.

The above results imply a remarkable promotion effect on the HER performance of Ni nanoparticles due to the surface modification effect. Indeed, the performance of the Ni-MOF derived HER catalysts is very sensitive to their surface state. Either large excess of carbon (Ni-Ar) or over attenuated carbon coating (Ni-0.4NH_3) results deterioration of the HER performance. Such sensitive dependence on the surface carbon coating is in agreement with a recent theoretical study by Deng et al [14], which suggested that thin graphene coating on Ni-Co nanoparticles can promote the HER activity by modulating the binding energy with the atomic H, while this promotion effect rapidly diminishes as the number of the graphene layers increases. In addition, surface nitridation of Ni is also beneficial for HER, as the Ni-0.4NH_3 sample is far more active than metallic Ni particles with similar size. To the best of our knowledge, the effect of surface nitridation of Ni on its HER activity has not been clearly addressed yet. An interesting issue is whether the surface nitrodation and carbon coating have synergism in promoting HER, which needs to be clarified with further study.

The strong carbon removal effect of NH_3 during the pyrolysis of the Ni-MOF $Ni_2(bdc)_2(ted)$ is critical to obtain the desired surface state for HER. To understand this effect, comparative experiments are carried out. The role of the reactive H species is first studied. As shown in Table 1, the sample obtained by pyrolysis in H_2 also contains high carbon content (30.56 wt%). TEM study also shows that the Ni-0.2H_2 sample shows very similar morphology to that of Ni-Ar, i.e. Ni particles embedded in a continuous carbon matrix (Fig. S3). Therefore, the carbon removal effect is not due to the reactive H species. Another conclusion is that NH_3 can only eliminate carbon before the organic ligands become fully carbonized. In another comparative experiment, the Ni-Ar sample is further treated in NH_3 at 560 °C for 1 h. However, there is little structure change observed (Fig. S3). The carbon content remains above 30 wt% (Table 1). Therefore, NH_3 treatment barely shows any carbon removal effect for well carbonized materials. This is in agreement with previous results[38, 42, 43]. It should be emphasized that the carbon removal effect and the subsequent surface state of Ni particles are also strongly associated with the ligand and the topology of the Ni-MOFs. Using other Ni-MOFs as the precursors is also possible, while the optimal condition for the treatment may vary.

A possible carbon removal mechanism is that NH_3 can cleave the C-C bonds in the organic ligands at high temperature, yielding smaller, more volatile molecules. In well carbonized materials, each carbon atoms are connected to three or four neighbouring carbon atoms in the network. Formation of volatile small molecules becomes more difficult in this case. In recent years, there is an increasing interest in deriving functional materials by pyrolysis of MOFs. This unique carbon removal effect of NH_3 during pyrolysis of MOFs has not been reported previously. We believe it will further advance the booming research field of MOFs derived functional materials.

Conclusions

We demonstrate that controlled pyrolysis of the MOF structure $Ni_2(bdc)_2(ted)$ in NH_3 atmosphere yields Ni nanoparticles with surface nitridation and thin carbon layer coating. The surface modified Ni nanoparticles exhibit one of the highest activity for HER among the Ni based noble metal free HER catalysts reported so far. The remarkable promotion effect due to surface modification will assist the development of low cost HER catalysts to support the renewable hydrogen generation by water electrolysis.

Acknowledgements

This study is supported by National Natural Science Foundation of China (No. U1201241, 11375020, 51431001 and 21321001).

Notes and references

1. C. G. Morales-Guio, L. A. Stern and X. L. Hu, *Chem. Soc. Rev.*, 2014, **43**, 6555-6569.
2. P. C. K. Vesborg, B. Seger and I. Chorkendorff, *J. Phys. Chem. Lett.*, 2015, **6**, 951-957.
3. W. F. Chen, J. T. Muckerman and E. Fujita, *Chem. Comm.*, 2013, **49**, 8896-8909.
4. R. Gazey, S. K. Salman and D. D. Aklil-D'Halluin, *J. Power Sources*, 2006, **157**, 841-847.
5. Ø. Ulleberg, T. Nakken and A. Eté, *Int. J. Hydrogen Energy*, 2010, **35**, 1841-1852.
6. G. Weidong and Y. Zhuoyong, *Int. J. Hydrogen Energy*, 2012, **37**, 737-740.
7. B. A. Pinaud, J. D. Benck, L. C. Seitz, A. J. Forman, Z. Chen, T. G. Deutsch, B. D. James, K. N. Baum, G. N. Baum, S. Ardo, H. Wang, E. Miller and T. F. Jaramillo, *Energy Environ. Sci.*, 2013, **6**, 1983-2002.
8. J. R. McKone, B. F. Sadtler, C. A. Werlang, N. S. Lewis and H. B. Gray, *ACS Catal.*, 2013, **3**, 166-169.
9. Y. Liu, G. D. Li, L. Yuan, L. Ge, H. Ding, D. Wang and X. Zou, *Nanoscale*, 2015, **7**, 3130-3136.
10. Y. Wang, G. Zhang, W. Xu, P. Wan, Z. Lu, Y. Li and X. Sun, *ChemElectroChem*, 2014, **1**, 1138-1144.
11. Z. Yin and F. Chen, *J. Power Sources*, 2014, **265**, 273-281.
12. M. K. Bates, Q. Jia, N. Ramaswamy, R. J. Allen and S. Mukerjee, *J. Phys. Chem. C*, 2015, **119**, 5467-5477.
13. I. Herraiz-Cardona, C. González-Buch, C. Valero-Vidal, E. Ortega and V. Pérez-Herranz, *J. Power Sources*, 2013, **240**, 698-704.
14. J. Deng, P. Ren, D. Deng and X. Bao, *Angew. Chem. Int. Ed.*, 2015, **54**, 2100-2104.
15. N. Danilovic, R. Subbaraman, D. Strmcnik, K. C. Chang, A. P. Paulikas, V. R. Stamenkovic and N. M. Markovic, *Angew. Chem. Int. Ed.*, 2012, **51**, 12495-12498.
16. M. Gong, W. Zhou, M. C. Tsai, J. Zhou, M. Guan, M. C. Lin, B. Zhang, Y. Hu, D. Y. Wang, J. Yang, S. J. Pennycook, B. J. Hwang and H. Dai, *Nat. Commun.*, 2014, **5**, 4695.
17. E. J. Popczun, J. R. McKone, C. G. Read, A. J. Biacchi, A. M. Wiltrout, N. S. Lewis and R. E. Schaak, *J. Am. Chem. Soc.*, 2013, **135**, 9267-9270.
18. P. Jiang, Q. Liu and X. Sun, *Nanoscale*, 2014, **6**, 13440-13445.
19. D. Kong, J. J. Cha, H. Wang, H. R. Lee and Y. Cui, *Energy Environ. Sci.*, 2013, **6**, 3553-3558.
20. N. Jiang, L. Bogoev, M. Popova, S. Gul, J. Yano and Y. Sun, *J. Mater. Chem. A*, 2014, **2**, 19407-19414.
21. C. Ouyang, X. Wang, C. Wang, X. Zhang, J. Wu, Z. Ma, S. Dou and S. Wang, *Electrochimica Acta*, 2015, **174**, 297-301.
22. X. Wang, J. Zhou, H. Fu, W. Li, X. Fan, G. Xin, J. Zheng and X. Li, *J. Mater. Chem. A*, 2014, **2**, 14064-14070.
23. Y. Song, X. Li, L. Sun and L. Wang, *RSC Adv.*, 2014, **5**, 7267-7279.
24. W. Chaikittisilp, K. Ariga and Y. Yamauchi, *J. Mater. Chem. A*, 2013, **1**, 14-19.
25. W. Xia, J. H. Zhu, W. H. Guo, L. An, D. G. Xia and R. Q. Zou, *J. Mater. Chem. A*, 2014, **2**, 11606-11613.
26. T. Tian, L. Ai and J. Jiang, *RSC Adv.*, 2015, **5**, 10290-10295.
27. B. Arstad, H. Fjellvag, K. O. Kongshaug, O. Swang and R. Blom, *Adsorpt.-J. Int. Adsorpt. Soc.*, 2008, **14**, 755-762.
28. P. Song, Y. Li, B. He, J. Yang, J. Zheng and X. Li, *Microporous Mesoporous Mat.*, 2011, **142**, 208-213.
29. S. Ma, G. A. Goenaga, A. V. Call and D. J. Liu, *Chem. Eur. J.*, 2011, **17**, 2063-2067.
30. R. Das, P. Pachfule, R. Banerjee and P. Poddar, *Nanoscale*, 2012, **4**, 591-599.
31. A. Banerjee, R. Gokhale, S. Bhatnagar, J. Jog, M. Bhardwaj, B. Lefez, B. Hannoyer and S. Ogale, *J. Mater. Chem.*, 2012, **22**, 19694-19699.
32. T. Fu, M. Wang, W. Cai, Y. Cui, F. Gao, L. Peng, W. Chen and W. Ding, *ACS Catal.*, 2014, **4**, 2536-2543.
33. Z. Zhao, H. Wu, H. He, X. Xu and Y. Jin, *Adv. Funct. Mater.*, 2014, **24**, 4698-4705.
34. B. Cao, G. M. Veith, J. C. Neuefeind, R. R. Adzic and P. G. Khalifah, *J. Am. Chem. Soc.*, 2013, **135**, 19186-19192.
35. Y. Zheng, Y. Jiao, L. H. Li, T. Xing, Y. Chen, M. Jaroniec and S. Z. Qiao, *ACS Nano*, 2014, **8**, 5290-5296.
36. Y. Zheng, Y. Jiao, Y. Zhu, L. H. Li, Y. Han, Y. Chen, A. Du, M. Jaroniec and S. Z. Qiao, *Nat. Commun.*, 2014, **5**, 3783.
37. W. F. Chen, C. H. Wang, K. Sasaki, N. Marinkovic, W. Xu, J. T. Muckerman, Y. Zhu and R. R. Adzic, *Energy Environ. Sci.*, 2013, **6**, 943-951.
38. W. F. Chen, K. Sasaki, C. Ma, A. I. Frenkel, N. Marinkovic, J. T. Muckerman, Y. Zhu and R. R. Adzic, *Angew. Chem. Int. Ed.*, 2012, **51**, 6131-6135.
39. L. Tao, X. Duan, C. Wang, X. Duan and S. Wang, *Chem. Comm.*, 2015, **51**, 7470-7473.
40. H. Vrubel and X. Hu, *Angew. Chem. Int. Ed.*, 2012, **51**, 12703-12706.
41. M. A. McArthur, L. Jorge, S. Coulombe and S. Omanovic, *J. Power Sources*, 2014, **266**, 365-373.
42. J. Deng, P. Ren, D. Deng, L. Yu, F. Yang and X. Bao, *Energy Environ. Sci.*, 2014, **7**, 1919-1923.
43. X. Yang, G. Zhang, M. Zhong, D. Wu and R. Fu, *Langmuir*, 2014, **30**, 9183-9189.

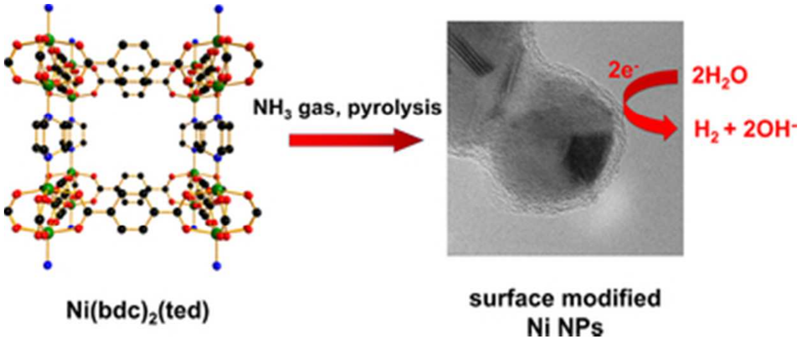

33x14mm (300 x 300 DPI)